SAND2020-5494

Sandia National Laboratories

SANDIA REPORT

SAND2020-5274

Printed May 2020

Sterilization of N95 Respirators via Gamma Radiation: Comparison of Post-sterilization Efficacy

Paul M. Thelen, Anne M. Grillet, Martin B. Nemer, Haedi E. DeAngelis, Maryla A. Wasiolek, Don J. Hanson, Mark E. Stavig, Michael A. Omana, Andres L. Sanchez, David W. Vehar

Prepared by
Sandia National Laboratories
Albuquerque, New Mexico
87185 and Livermore,
California 94550

Sandia
National
Laboratories

Issued by Sandia National Laboratories, operated for the United States Department of Energy by National Technology & Engineering Solutions of Sandia, LLC.

Available to DOE and DOE contractors from

U.S. Department of Energy

Office of Scientific and Technical Information

P.O. Box 62

Oak Ridge, TN 37831

Telephone: (865) 576-8401

Facsimile: (865) 576-5728

E-Mail: reports@osti.gov

Online ordering: http://www.osti.gov/scitech

Available to the public from

U.S. Department of Commerce

National Technical Information Service

5301 Shawnee Rd

Alexandria, VA 22312

Telephone: (800) 553-6847

Facsimile: (703) 605-6900

E-Mail: orders@ntis.gov

Online order: https://classic.ntis.gov/help/order-methods/

ABSTRACT

OBJECTIVE

This study evaluated gamma irradiation for sterilization and reuse of two models of N95 respirators after gamma radiation sterilization as a method to increase availability of N95 respirators during a shortage.

METHODS

The Sandia National Laboratories Gamma Irradiation Facility was used to irradiate two different models of N95 filtering facepiece respirators at doses ranging from 0 kGy(tissue) to 50 kGy(tissue). The following tests were used to determine the efficacy of the respirator after irradiation sterilization: Ambient Aerosol Condensation Nuclei Counter Quantitative Fit Test, tensile test, strain cycling, oscillatory dynamic mechanical analysis, microscopic image analysis of fiber layers, and electrostatic field measurements.

RESULTS

Both of the respirator models exhibited statistically significant changes after gamma irradiation as shown by the Quantitative Fit Test, electrostatic testing and the aerosol testing. The change in electrostatic charge of the filter was correlated with a reduction in capturing particles near the 200 nm size by approximately 40-50%.

CONCLUSION

Both tested respirators showed statistically significant changes associated with gamma sterilization. However, our results indicate that choices in materials and manufacturing methods to achieve N95 filtration lead to different magnitudes of damage when exposed to gamma radiation at sterilization relevant doses. This damage results in lower filtration performance. While our sample size (2 different types of respirators) was small, we did observe a change in electrostatic properties on a filter layer that coincided with the failure on the Quantitative Fit Test and reduction in aerosol filtering efficiency.

Key Words: N95 respirators, respirators, airborne transmission, pandemic prevention, COVID-19, gamma sterilization

ACKNOWLEDGEMENTS

This project addresses a complex, multidisciplinary problem that requires expertise in radiation, industrial hygiene, biology, biosafety, radiation metrology, bioaerosol, electrostatics, mechanical testing, and material science. These individuals played a key role in tackling this problem:

Adrianna Woltman, Melissa Finley, Rick Lykins, Eric Cook, Dora Wiemann, Taylor Settecerri, Ann Dallman, Darren Branch, Joel Harding, Michael Svinarich, Lorenzo Gutierrez, Tom Kulp, Chris Mckean, Josh Nolker, Steve Iveson, Matt Burger, Pat Griffin, Charles Barbour, Gil Herrera, Wahid Hermina, Nathan Price

CONTENTS

LIST OF FIGURES

LIST OF TABLES

This page left blank

ACRONYMS AND DEFINITIONS

Abbreviation	Definition
CDC	Centers for Disease Control and Prevention
CFR	Code of Federal Regulations
CNC	condensation nuclei counter
CPC	condensation particle counter
COVID-19	coronavirus disease 2019
DMA	differential mobility analyzer
EPR	electron paramagnetic resonance
FPT	filter penetration testbed
GIF	Gamma Irradiation Facility
Gy/s	gray per second
HDR	high dynamic range
kGy	kilogray
kV/inch	kilovolt per inch
LDRD	laboratory directed research and development
MeV	mega-electron volt
NIOSH	National Institute for Occupational Safety and Health
NIST	National Institute of Standards and Technology
OSHA	Occupational Safety and Health Administration
PPE	personal protective equipment
QNFT	quantitative fit test
SARS-CoV	severe acute respiratory syndrome coronavirus

1. INTRODUCTION AND BACKGROUND

The Coronavirus Disease 2019 (COVID-19) pandemic has strained healthcare systems and has led to a shortage of personal protective equipment (PPE). PPE is crucial to protect healthcare workers and maintain the highest quality patient care and surge capacity. Various non-traditional solutions are being proposed to relieve the shortage, such as PPE sterilization and reuse, fabric face masks, and 3D-printed equipment (1-3). Health care systems will likely employ various methods to address the PPE shortage based on their resources and capabilities.

Gamma sterilization is a commonly used method for sterilization of medical equipment (4). During this pandemic, gamma sterilization of PPE has been proposed (5). Gamma sterilization has been shown to inactivate many pathogens, including the Severe Acute Respiratory Syndrome Coronavirus 1 (SARS-CoV-1) at a dose of 10 kGy(tissue), although our literature review has not shown data specific to the inactivation dose of SARS-CoV-2, the virus that causes COVID-19 (6). Gamma sterilization has two key benefits for this application: high volumetric throughput on the order of a thousand respirators per hour per facility and the penetration ability that will sterilize objects without removing them from their packaging or container. This minimizes exposure to personnel during transportation and sterilization of contaminated material.

However, due to the nature of gamma radiation, caution must be used when sterilizing sensitive PPE, such as surgical-grade N95 respirators. N95 respirators come in many brands and models that use different materials and methods to meet industry specified filtration requirements. Most N95 respirators use a non-woven polymer fiber fabric as a filter, and some use an electret material that employs electrostatic forces to increase particle capture. Gamma radiation is known to modify the structure and properties of polymers and can adversely affect the filter materials in several ways, such as enhanced polymer oxidation, polymer chain scission or cross-linking , and electret material neutralization (7, 8).

The key contribution of this study is an assessment of the mechanical integrity and filtration properties of the two available models of respirators that were studied both before and after exposure to various doses of gamma radiation. Because of the limited sample size used in our study, we only refer to these two respirators as “model 1” and “model 2”. If this study is extended to address a wider assortment of respirator model and a larger sample size, the mapping of these designations to specific vendors can be made available. Efficacy data was collected through ambient aerosol condensation nuclei counter (CNC) quantitative fit testing (QNFT), mechanical testing of the elastic straps, microscopy, aerosol penetration testing and electric field measurements of each layer of the respirators. The data collected in this study can impact the decision to use gamma sterilization as a method of N95 reuse and guide future testing of other makes and models of N95 respirators.

2. METHODS

2.1. Radiation Source

In this effort, we irradiated 2 models of N95 respirators (Figure 2-1) at the Sandia National Laboratories Gamma Irradiation Facility (GIF)(9). This facility uses the cobalt-60 isotope to produce 1.17 and 1.33 MeV photons (Figure 2-2). The dose rate provided by this facility can be as high as 40 Gy(CaF_2)/s; however, for this effort we stayed below 0.5 Gy(CaF_2)/s to minimize material heating. The following doses for irradiation were targeted for this study:

- 0.0 kGy(tissue)
- 5.0 kGy(tissue)
- 10. kGy(tissue)
- 25. kGy(tissue)
- 50. kGy(tissue)

10 kGy(tissue) has been shown to inactivate SARS-CoV-1 (6). ISO11137-2:2013 specifies methods to substantiate 25 kGy(tissue) as a dose for sterility of medical devices (4).

For this experiment, we chose to use the GIF's 30-pin planar array of cobalt-60 to maximize uniformity of the dose. This geometry is most representative of commercial panoramic irradiators. This facility also has the ability to irradiate the samples in inert gas atmospheres. Some samples were irradiated in argon gas to assess the presence of oxidation-based effects.

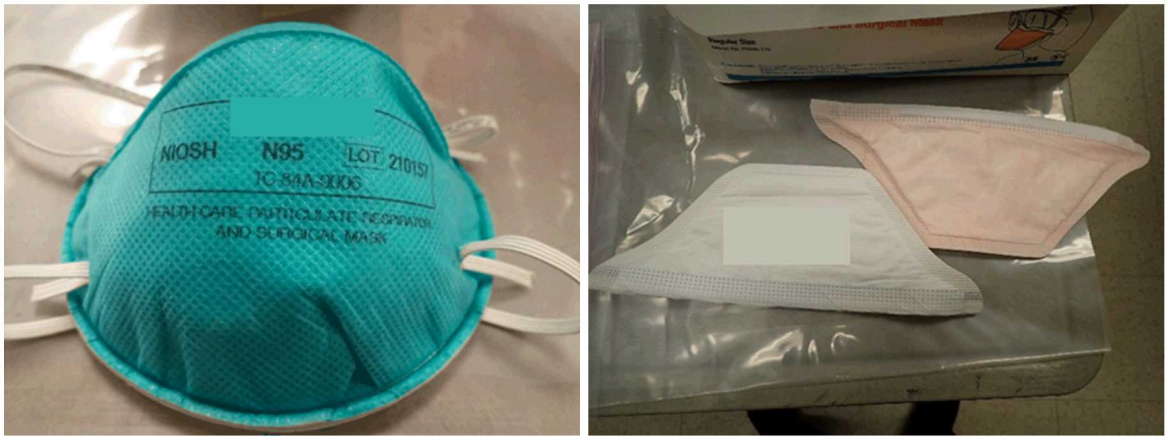

Figure 2-1. Two different models of N95 respirators. A cup shaped model referred to as Model 1 in this document (left) and a pouch/duck-bill model referred to as Model 2 in this document (right).

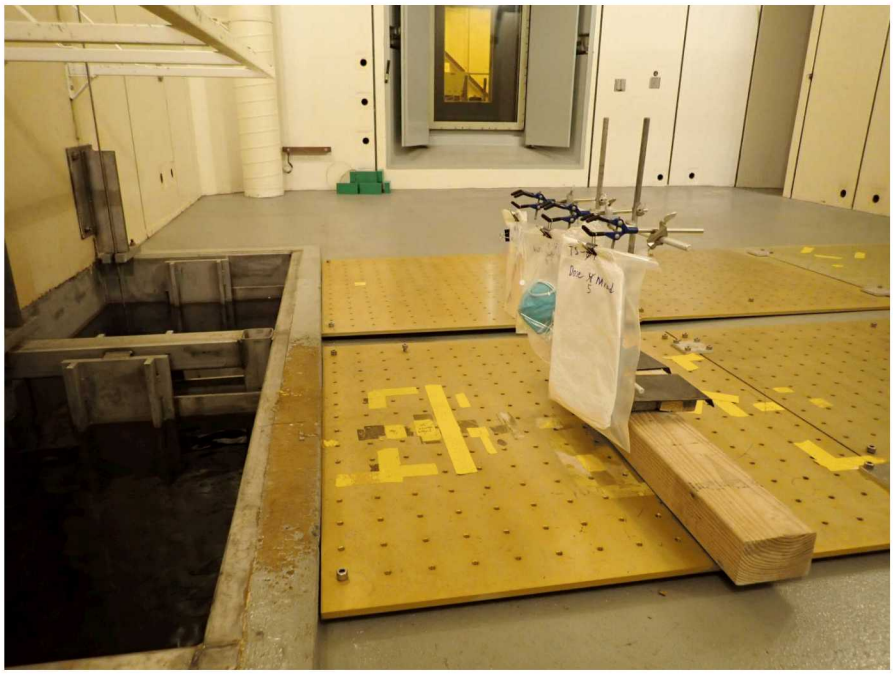

Figure 2-2. N95 respirators and other PPE arranged in the GIF. A planar cobalt-60 source is raised up from the pools on the left.

2.2. Dosimetry

Target doses were reached using a combination of duration and dose rate as measured by an ionization chamber (first column of Table 2-1). The actual dose was confirmed using alanine dosimetry (fifth column of Table 2-1). Note that throughout this document, dose is specified as a targeted tissue dose. The alanine dosimetry shows that we exceeded the targets consistently to ensure we do not underestimate the degradation caused by gamma radiation.

Three National Institute of Standards and Technology (NIST) traceable alanine dosimeters, nominally 65 mg, were irradiated in equilibrated vials with each set of respirators. Evaluation of absorbed dose was done by Electron Paramagnetic Resonance (EPR) spectroscopy using a Bruker ELEXSYS E500 spectrometer. Measured signal as compared to a reference pellet by spectral titration to normalize for environmental conditions in the resonance cavity at the time of measurement. This technique yields a measurement precision of approximately 1% and overall measurement uncertainties within 5% (1σ). The term titration in Table 2-1 refers to spectral titration, which is referring EPR measurements to a reference; in this case, another alanine pellet.

Two sets of respirators were irradiated at 25 kGy(tissue). The extra set of respirators at 25 kGy was used for aerosol penetration testing.

Table 2-1. Alanine Dosimetry Measurements

Target Dose ($kGy(CaF_2:Mn)$)	Pellet ID	Estimated Dose (kGy Tissue)	Titration	Measured Dose (kGy(Tissue))	Estimated Uncertainty of Measured Dose
10	1	11.3	121.86	11.5	4.2%
	2	11.3	122.61	11.5	4.2%
	3	11.3	122.17	11.5	4.2%
25	1	28.4	281.46	28.5	4.2%
	2	28.4	279.41	28.2	4.2%
	3	28.4	278.33	28.1	4.2%
25	1	28.4	274.27	27.6	4.2%
	2	28.4	271.99	27.3	4.2%
	3	28.4	270.26	27.0	4.2%
50	1	56.7	474.83	60.3	4.2%
	2	56.7	471.87	59.7	4.2%
	3	56.7	474.17	60.2	4.2%

2.3. Quantitative Fit Test

An Ambient Aerosol Condensation Nuclei Counter (CNC) Quantitative Fit Test (QNFT) was used to measure respirator efficacy. This test follows the Centers for Disease Control and Prevention's National Institute for Occupational Safety and Health (NIOSH) laboratory performance evaluation of N95 filtering facepiece respirators (10). The purpose of this performance evaluation is to meet the Occupational Safety and Health Administration (OSHA) Respiratory Protection Standard protocols as stated in 29 Code of Federal Regulation (CFR) 1910.134 (11). The TSI PortaCount Pro+ Respirator Fit Tester Model 8038 was used to carry out this test using the settings for N95 respirators (Figure 2-3). This device combines the filter penetration, seal integrity, and appropriate donning into a single quantitative score (Figure 2-4). A minimum score of 100 is needed for a half-mask respirator, such as the N95. For comparison, a respirator that has the external seal broken by inserting 2 fingers scored a fit factor of 3. The Industrial Hygiene team at Sandia National

Laboratories ensure correct donning to minimize that impact on the score. Scores lower than 100 on pristine respirators are not uncommon (12). The purpose of the QNFT for our application is to determine if there is a statistically significant change after radiation exposure.

The PortaCount operates by counting particles of various sizes generated by an aerosol source. Particles are measured on either side of the respirator. A tube penetrates the respirator through a seal, and a second tube is left open just outside of the respirator. The difference in measurement between these tubes under various conditions is correlated by the PortaCount into a quantitative score of respirator performance.

Figure 2-3. TSI PortaCount Pro+ Respirator Fit Tester Model 8038

Figure 2-4. N95 respirator being tested by the PortaCount. The tester will provide a quantitative fit factor that scores the filtration efficacy, the respirator seal, and the ability of our industrial hygiene team to don the machine.

2.4. Mechanical Testing of Elastic Straps

A tensile test was performed using a TA Instruments RSA-G2 rheometer to measure non-linear properties of the elastic straps (Figure 2-5) (Figure 2-6). The main purpose of this test is to observe if the radiation could increase the likelihood of the straps breaking under normal strain conditions. Elastic tension in the straps is also critical to ensure the respirator achieves a seal to the wearers face. In order to maximize the effect, the test was performed on the control and the samples exposed to the highest dose of 50 kGy(tissue) for each respirator models. This test did not consider loss of mechanical integrity due to long duration use, nor multiple donning of each respirator which would also factor into mechanical degradation (13). The CDC has guidelines associated with these issues(14).

Figure 2-5. TA Instruments RSA-G2 Solid Analyzer

Figure 2-6. Respirator straps under tension for mechanical testing

Load-unload cycles and Oscillatory Dynamic Mechanical Analysis were performed on an Anton Paar Modular Compact TwinDrive rheometer to measure the linear extensional properties of the elastic straps (Figure 2-7). The main purpose of this test is to observe if the degradation rate of multiple donning of the straps is statistically different after radiation. Both respirator straps were placed in tension along the length of the strap. The loss and storage moduli were measured as a function of frequency and strain.

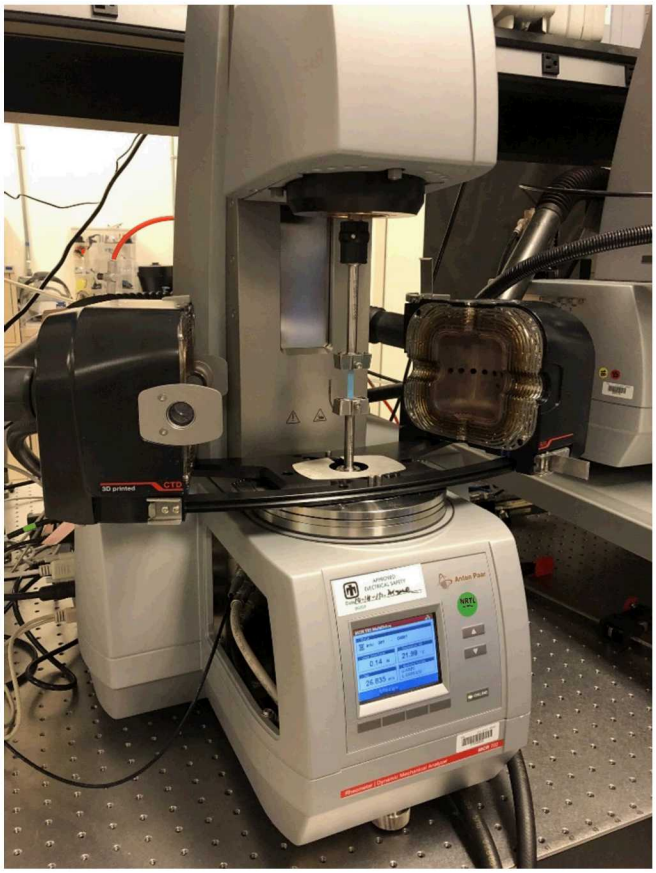

Figure 2-7. An Anton Paar Modular Compact TwinDrive rheometer taking measurements on a Model 2 elastic strap sample

2.5. Image Analysis of N95 Respirator Layers

A Keyence VHX6000 microscope was used to image each layer of each N95 respirator (Figure 2-8). To maximize visual differences, we compared the 0 kGy(tissue) control against the respirators that received 50 kGy(tissue). Layers that use fibers as a filtration mechanism had fiber diameter measured and compared to look for dimensional changes within the filters. 3D image reconstruction technology was used to allow for more fibers to be in focus for measurement. High Dynamic Range (HDR) improved image resolution by combining image data from multiple exposures to generate the image. HDR also allowed images at higher magnifications up to 1500x to be used for measurements. This is the only quantitative measurement performed by image analysis. All other observations are qualitative.

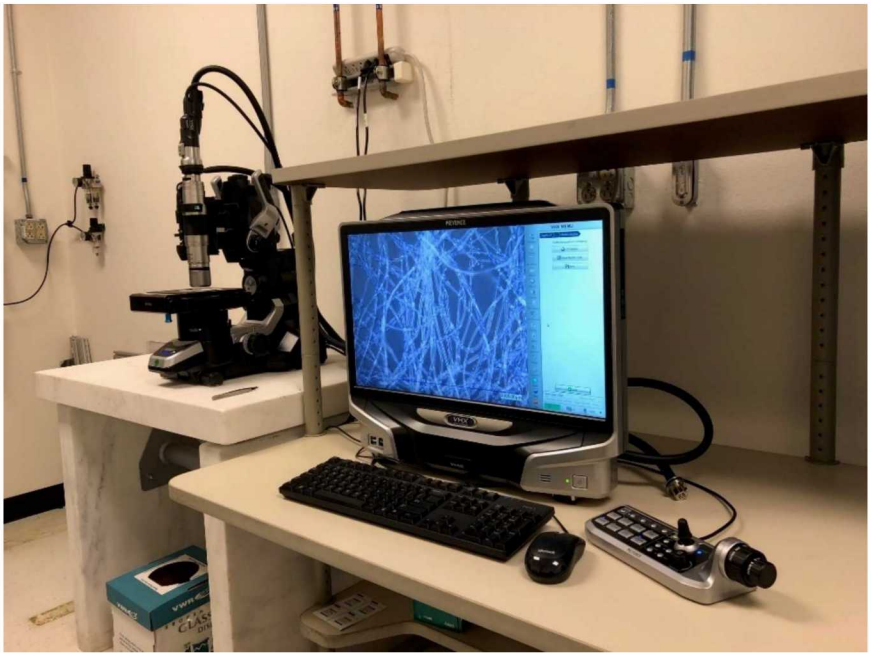

Figure 2-8. A Keyence VHX6000 microscope viewing a fibrous layer of a respirator

2.6. Electrostatic Potential Measurements

Many newer N95 respirators use an electret material to efficiently capture particles out of the air using electrostatic forces (15). Due to the ability of gamma radiation to neutralize electret materials, the purpose of this test is to have a quantifiable method of measuring this effect (7, 16)

An electrostatic field meter was used to measure the electric field strength near 1" outer diameter coupons punched from each respirator. The field meter, a Prostat PFM-711A hand-held field meter, although imprecise was utilized. The field meter was placed 0.7" away from an insulating surface on which samples were placed for measurement (Figure 2-9). This distance was chosen by checking repeatability and accuracy against a 1" outer diameter aluminum disc connected to a DC power supply. The field meter is designed for measuring larger areas. The field meter was grounded to an optical table on which the insulating surface sat. A Fluke 289 multimeter was used to verify that the insulated surface was not electrically connected to the field-meter ground.

Later in the project, we learned that the measurement method that we had used with the electrostatic field meter had drawbacks. Namely, placement of the coupon on the insulating surface

caused that surface to charge due to capacitance, decreasing the field measured by the electrostatic field meter. Regardless, the results are presented herein. To rectify this shortcoming, a Trek 821HH contact electrostatic voltmeter was also utilized with samples suspended above a grounded optical table, as shown in Figure 2-9 (bottom).

The 1" outer diameter aluminum disc, with an extended tab, was taped to the insulating surface in a location designated for coupon measurement. The aluminum disc was charged using a Keysight EA36030A ±20V DC power supply. The results showed reasonably consistent readings between the power supply, the field meter, and the electrostatic voltmeter. The field meter and coupons that were measured were both located in the same fixed positions. The aluminum disc was removed when measuring the field emitted by the coupons. The small circle with a centrally placed dot located on the insulating surface was a second reference point for the meter location. The meter emits two LEDs in a bullseye-like pattern for positioning the meter at the correct distance to the surface to be measured; that distance requirement (≈ 1") was intentionally violated herein for our measurement purposes.

With the field meter, each coupon was measured with the external surface facing the field meter and then subsequently with the internal surface facing the field meter. The reported difference result is the difference between these two measurements. We define the external surface as that facing away from the wearer, and internal surface as that facing the wearer. Repeat measurements were made on some layers.

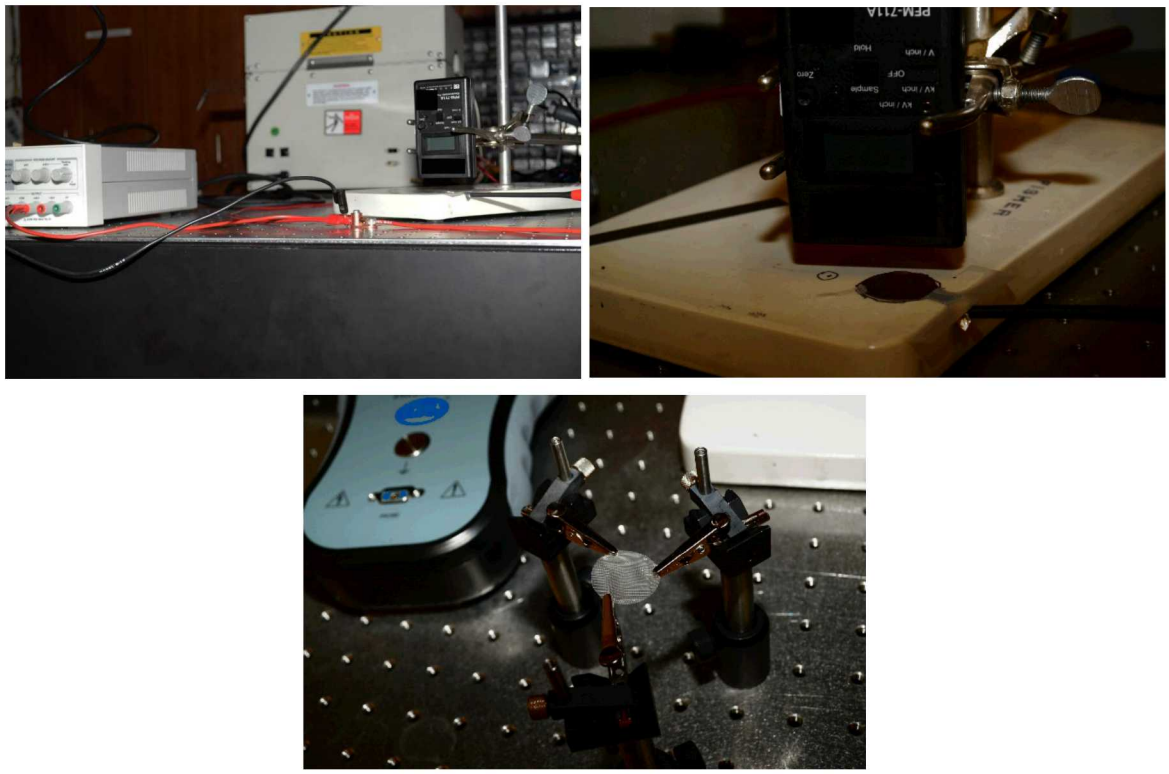

Figure 2-9. The electrostatic field meter measuring the field generated by a 1" outer diameter sample of either filter or charged aluminum disc (top). A contact electrostatic probe was also used with samples suspended above the grounded optical table (bottom).

2.7. Filtration Performance Testing

Two existing filtration systems were used to test the filtration performance of the respirators.

The first system is a large-scale filtration system designed to test commercial filter boxes. It has controlled laminar air flow, pressure, and sodium chloride (NaCl) aerosol concentration. Air is filtered and enters through a laminar flow element where pressure is measured via a pressure transducer. The air is passed through a high efficiency particulate air (HEPA) filter. The air then mixes with test aerosol of nano-sized particulates of NaCl dissolved in deionized water made using a Topas aerosol generator. A dilution loop regulated the concentration of the test aerosol. The test aerosol then passes through respirators mounted in a box. Pressure drop across the respirator is measured aerosol sampling probes measured the aerosol concentration on both the upstream and downstream of the respirator using a scanning mobility particle sizer spectrometer composed of an electrostatic classifier, differential mobility analyzer, and a condensation particle counter. The scanning system can collect data for particle sizes at low as 75 nm, the particle size referred to in NIOSH guidelines (17). Documented size distributions of SARS-CoV-2 aerosol range from of 250 nm to greater than 25 μm (18). Efficiency is calculated as the difference in concentration of 75 nm particles upstream of the mounted respirator and concentration downstream of the respirator divided by the concentration of particles upstream of the respirator.

The second system is a Filter Penetration Testbed (FPT). The testbed was designed to follow, when possible, NIOSH guidance and the CFR set forth in 42 CFR, Part 84, Subpart K, §84.181. The FPT performs filtration efficiency measurements on a monodisperse NaCl aerosol by utilizing a TSI 8020 Electrostatic Classifier and TSI 3081L Differential Mobility Analyzer (DMA) upstream from a 47 mm stainless filter housing. NIOSH guidance mentions an aerosol with particle size median diameter of 0.075 ± 0.020 μm with a geometric standard deviation not exceeding 1.86 that has been neutralized to the Boltzmann equilibrium state, which the FPT system measured. However, it is worth noting that the monodisperse aerosol does not capture the FDA recommended mass median particle diameter of 0.3 μm. Additionally, the filter housing diameter used by the FPT is smaller than the mounts used by TSI 8130 (120mm). Therefore, flow rates were adjusted according to equivalent filter face velocities, so geometry of the filter housing was mitigated. Finally, in order to calculate filter efficiency, concentration was measured upstream and downstream of the filter material tested by a TSI 8022 Condensation Particle Counter (CPC).

The pouch/duck-bill style respirator was tested on both systems. Due to the geometry of the cup-shaped respirator, only the FPT was used.

Figure 2-10. The pouch/duck-bill style respirator split and mounted into a filtration box for the large-scale filtration testbed

Figure 2-11. The stainless steel housing for a circular punch of respirator filter (left). The FPT system (right)

3. RESULTS

3.1. Quantitative Fit Test

The TSI PortaCount Pro Model 8038 produces a numerical score for the fit test known as a fit factor. The results of our test are shown below (Table 3-1).

Table 3-1. QNFT Results at various doses and argon backfill for both respirator models

	Dose (kGy(Tissue))					
Model	0.0	5.0	10.	25.	50.	50. + Ar
1	219	4	6	5	7	5
	176	6	5	7	7	5
2	36	16	15	14	21	13
	84	14	17	13	17	12

Due to limited N95 respirator supply, a larger statistical sample could not be gathered for this study. The irradiated respirators are distinct from the control respirator (respirators were not measured before irradiation), thus an unpaired t-test can be used to determine if there is a difference between the control and irradiated samples.

For the Model 1, the two-tailed P value is less than 0.0001; by conventional criteria, this difference is considered to be statistically significant. The mean difference is 192 (95% confidence interval from 174 to 210).

For the Model 2 respirator, the two-tailed P value is equal to 0.0004; by conventional criteria, this difference is considered to be statistically significant. The mean difference is 45 (95% confidence interval from 26 to 64).

Argon gas was used to backfill samples irradiated to 50 kGy(tissue) to determine if oxidation-based effects are prevalent. A larger, more diverse data set is needed for the Model 1 respirator because the standard deviation of the 50 kGy(tissue) and 50 kGy(tissue) + argon samples are zero and therefore, the t test cannot be performed. For the Model 2 respirator, the two-tailed P value is equal to 0.09; by conventional criteria, this difference is considered to be not statistically significant.

3.2. Mechanical Testing of Elastic Straps

The straps for both models of N95 respirators did not fail under strains up to 200% regardless of radiation dose. A 200% strain is tripling the length of the strap. The slight differences between irradiated and control straps is not significant for the purpose of respirator reuse (Figure 3-1) (Figure 3-2).

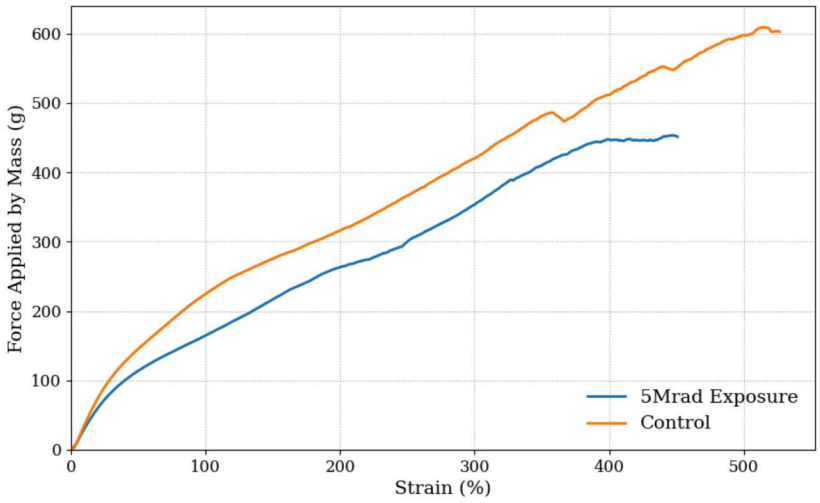

Figure 3-1. The Tensile Test results on the Model 2. The differences between the 0 kGy(tissue) and 50 kGy(tissue) samples is not substantial. An important observation is neither sample broke even at 200% strain, which is when the strap is three time it's original length.

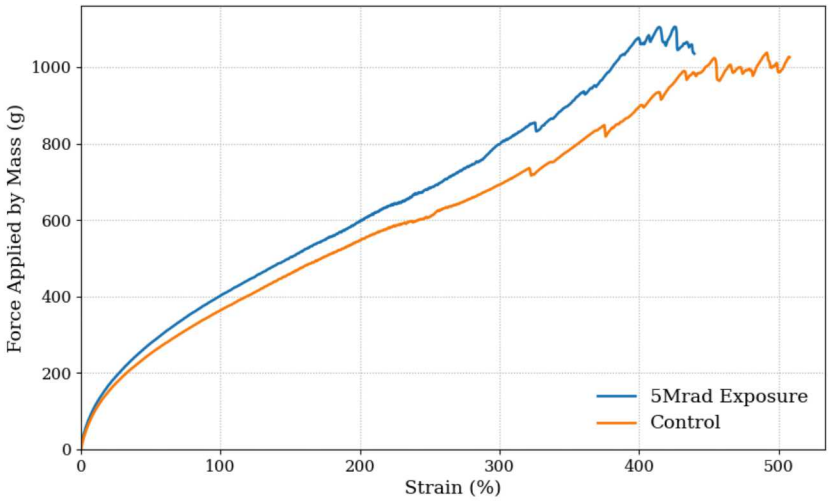

Figure 3-2. The Tensile Test results on the Model 1. The differences between the 0 kGy(tissue) and 50 kGy(tissue) samples is not substantial. An important observation is neither sample broke even at 200% strain, which is when the strap is three time it's original length.

Both N95 respirators do not return to their original length/strain after stress is applied. With only one sample at for each strain, there is not enough data to determine if differences are statistically significant between 0 kGy(tissue) and 50 kGy(tissue) samples (Figure 3-3).

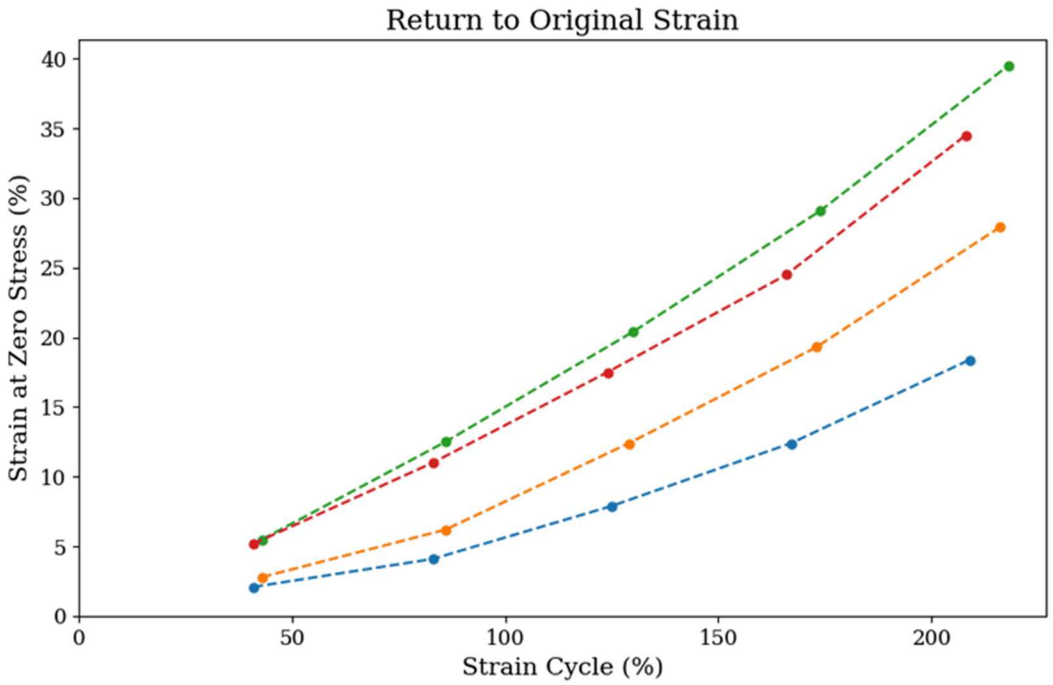

Figure 3-3. Green – Model 1 Control, Red – Model 1 at 50 kGy(tissue), Blue – Model 2 Control, Orange – Model 2 at 50 kGy(tissue). The return to original strain test results. The Model 2 respirator is more plastic than the Model 1 respirator and will remain at a longer length after being stretched.

The change in storage and loss extensional moduli were averaged over eleven measurements from 0.1 – 1% strain for each respirator at each dose and the average (and standard deviations in parentheses) are as follows: The Model 2 storage modulus changed by -8% (8%) and the loss modulus changed by -1% (4%). The Model 1 respirator storage modulus changed by 21% (3%) and the loss modulus changed by 14% (4%). Note that the measurements were taken from a single sample from each respirator, so these errors do not account for deviations in respirator lot (Figure 3-4) (Figure 3-5) (Figure 3-6) (Figure 3-7). To summarize, there were not substantial differences in the storage modulus and loss modulus when comparing the 50 kGy(tissue) samples against the 0 kGy(tissue) control for the Model 2 respirator. There was a statistically significant difference in the moduli for the Model 1 respirator; however, the difference is likely not great enough to have a practical impact.

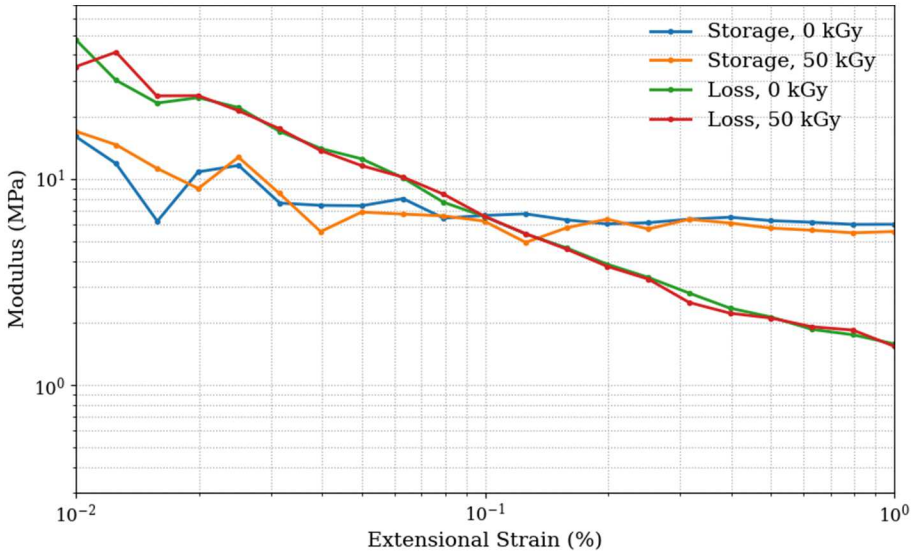

Figure 3-4. The strain dependent storage and loss moduli for the Model 2 respirator. The eleven samples taken at each dose do not show a statistically significant difference between the control and irradiated straps.

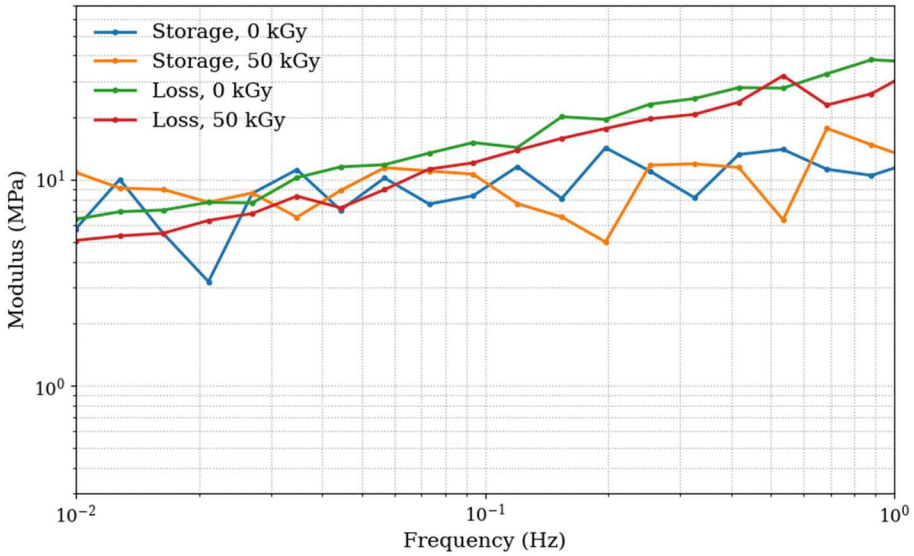

Figure 3-5. The frequency dependent storage and loss moduli for the Model 2 respirator. The eleven samples taken at each dose do not show a statistically significant difference between the control and irradiated straps.

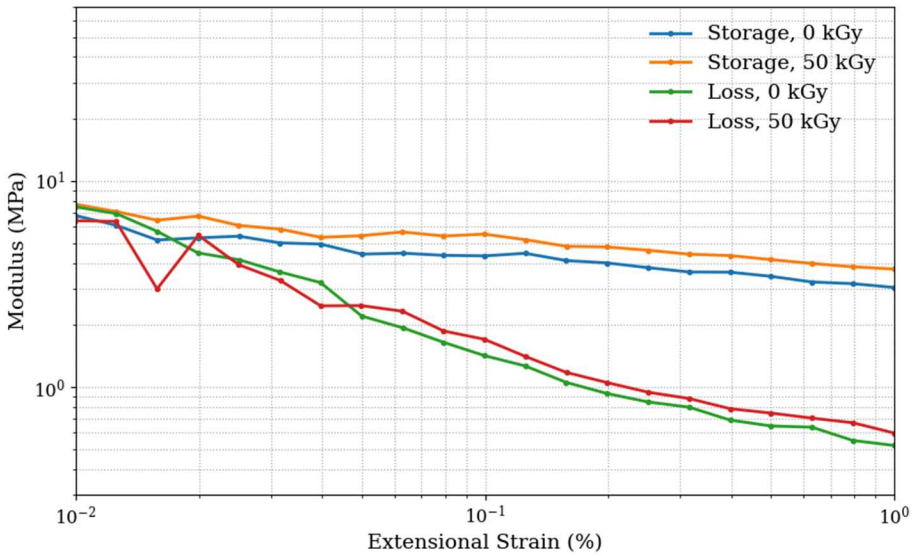

Figure 3-6. The strain dependent storage and loss moduli for the Model 1 respirator. The eleven samples taken at each dose show a small, but statistically significant difference between the control and irradiated straps.

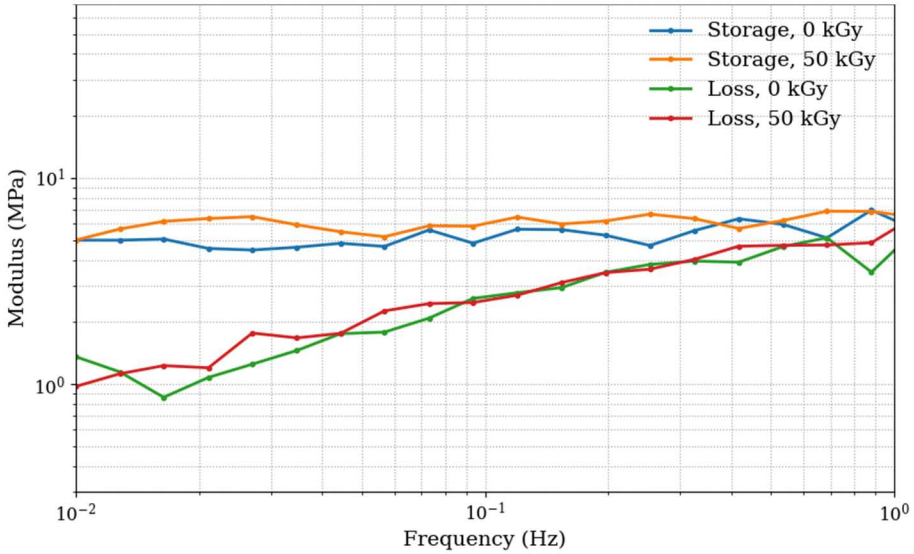

Figure 3-7. The frequency dependent storage and loss moduli for the Model 1 respirator. The eleven samples taken at each dose show a small, but statistically significant difference between the control and irradiated straps.

Both the respirator model straps are viscoelastic as shown by the similar storage and loss moduli. Both the moduli measurements and the strain at zero stress measurements show that the Model 1 material recovers more deformation when stretched. The Model 2 material is stiffer (higher moduli) and more plastic, which means it experiences more unrecoverable plastic deformation from use to use. This may limit the number of donnings that are possible with this respirator.

3.3. Image Analysis of N95 Respirator Layers

The 0 and 50 kGy(tissue) respirator samples of both respirator types were analyzed with a Keyence digital microscope. 1" outer diameter punches were taken from the respirator for analysis. The

Model 2 N95 respirator is comprised of five layers of material. The Model 1 N95 respirator is comprised of four layers (Figure 3-8).

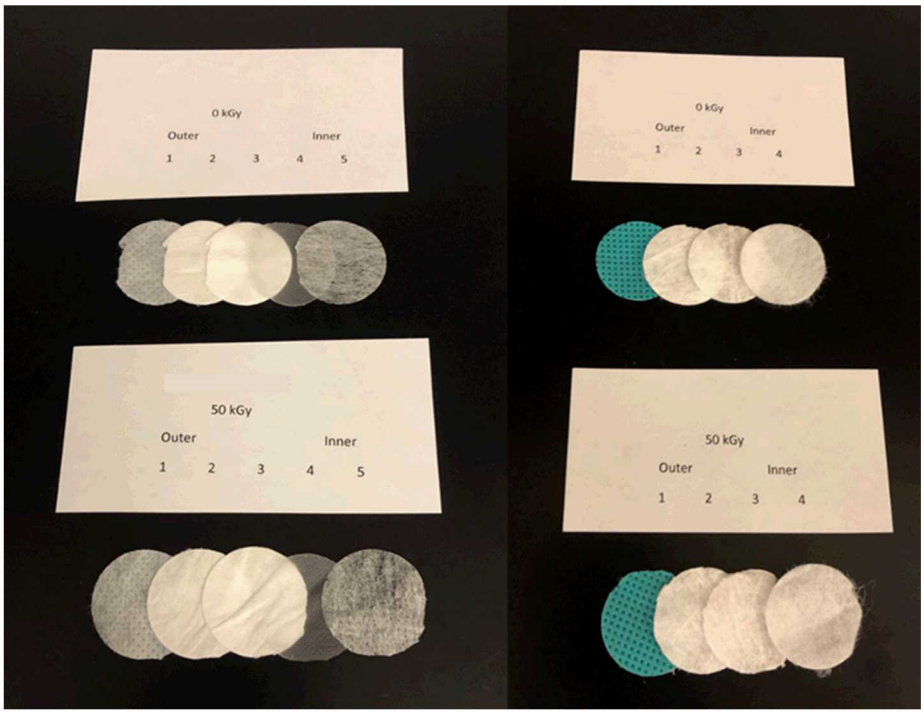

Figure 3-8. 1" diameter punches of each layer on each respirator. There are five layers in the Model 2 respirators (left two samples) and four layers in the Model 1 respirators (right two samples). Image analysis was performed on 0 kGy(tissue) samples (top two samples) and 50 kGy(tissue) (bottom two samples).

The average measured fiber diameter (and standard deviations in parentheses) are given below (Table 3-2) (Table 3-3). Note that the 4th layer on the Model 2 respirator does not have a fiber like structure that can be measured for diameter. Within the error of measurement, there is no significant change in fiber size for either respirator after irradiation. An example of HDR enhanced fiber diameter measurement is given below (Figure 3-9). No statistically significant fiber size or fabric morphology differences were observed in any sample after gamma irradiation. Additional images can be found in 0.

Table 3-2. Fiber diameter measurements for Model 2 respirator layers

Layer	0 kGy(tissue) diameter in μm	50 kGy(tissue) diameter in μm
1	18.2 (0.8)	17.5 (1.0)
2	2.5 (0.7)	2.8 (1.2)
3	2.5 (0.8)	3.2 (1.2)
5	20.1 (2.5)	21.2 (1.5)

Table 3-3. Fiber diameter measurements for the Model 1 respirator layers

Layer	0 kGy(tissue) diameter in µm	50 kGy(tissue) diameter in µm
1	19.9 (0.9)	21.3 (2.4)
2	2.6 (1.2)	3.1 (1.5)
3	3.2 (1.8)	3.1 (1.7)
4	20.6 (2.3)	22.4 (1.8)

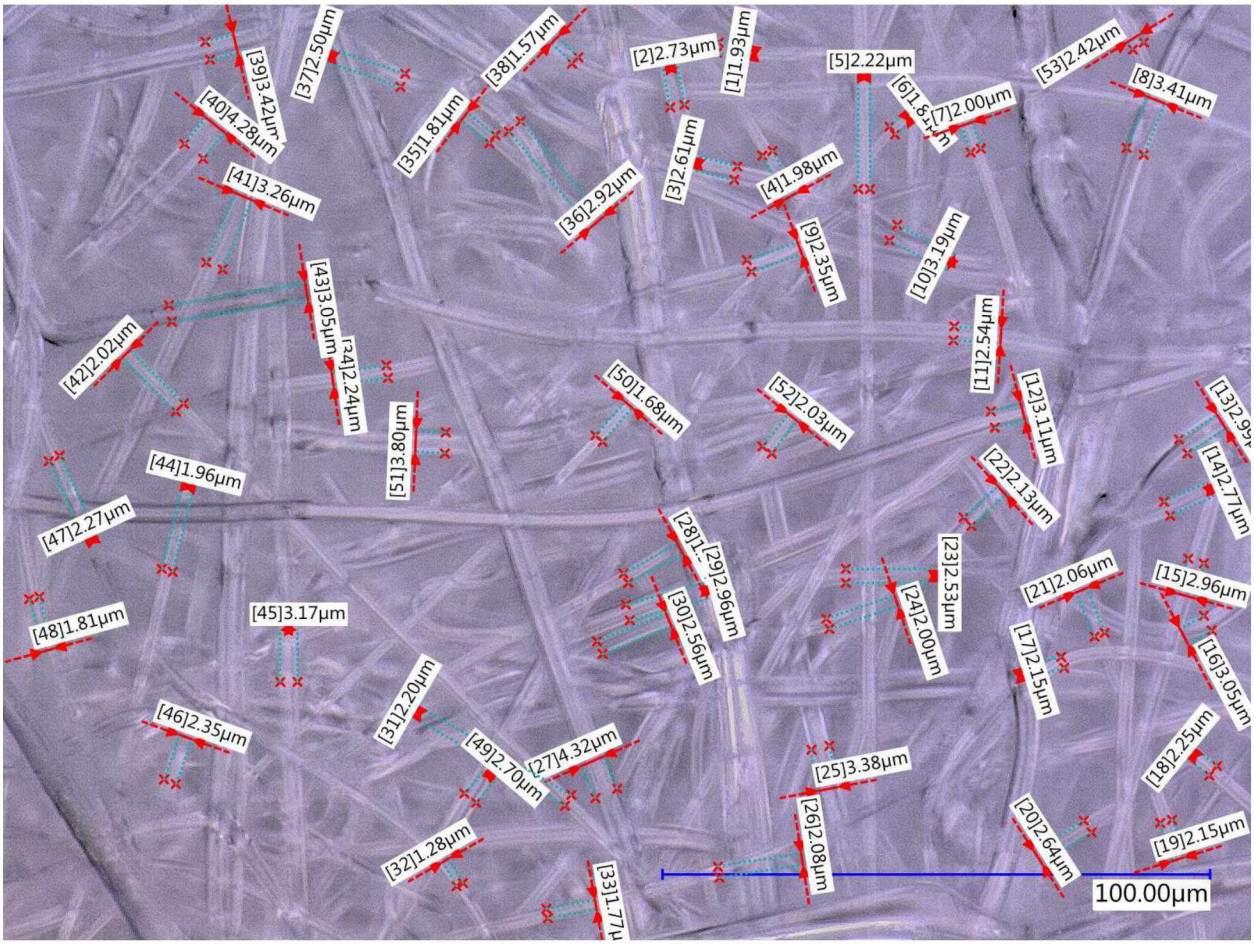

Figure 3-9. An example of how HDR improves fiber diameter measurements taken on the microscope

3.4. Electrostatic Filter Measurements

The electrostatic field emitted from the 1" outer diameter punches were measured. The data in Table 3-4 shows the results for the average and difference in the electrostatic field between the external and internal surface of each coupon, as measured with the electrostatic field meter. The data in Table 3-5 shows the results from the electrostatic volt meter. Both methods (field meter versus the electrostatic volt meter) had significant variability in the measurements as shown by the standard deviations of the measurement in both tables. Significant variability in field measurements

is consistent with other literature measurements of electret materials (19). While the absolute values are uncertain, we are confident that the two methods qualitatively detected changes in the charge state of the respirator layers before and after exposure to gamma radiation.

Both respirator models have what appears to be a pair of fine fiber layers in their core that are believed to be the primarily means of filtration. While making electrostatic measurements with the electrostatic field meter, this pair of layers was kept intact, measuring both sides of the pair. Electrostatic field testing prior to gamma irradiation showed that the pair had significant electrostatic potential and that the two sides of this layer were oppositely charged. These measurements, shown in Table 3-4, show a difference measurement (difference between the two sides of the pair) of 0.9 kV/inch was measured from the 0 kGy(tissue) Model 1 sample. This decreased to 0.1 kV/inch after exposure to a gamma radiation dose of 50 kGy(tissue). Measurements from the Trek 821HH contact field meter, shown in Table 3-5, were performed by peeling the pair of the fine-fiber core layers apart. From the Trek 821HH measurements, it was found that both respirators had significant changes to the electrostatic fields of the fine-fiber pair before and after exposure to gamma radiation. From the contact electrostatic field measurements, it appears that the positively charged filtration layers in both respirators changed their sign after exposure to gamma radiation.

Table 3-4. Electrostatic field measurement of various layers within respirators. Layers 2 and 3 were measured together on the Model 1 respirator. Standard deviation given in parenthesis.

Models	Layer	Average 0 kGy(tissue) (kV/in)	Average 50 kGy(tissue) (kV/in)	Difference 0 kGy(tissue) (kV/in)	Difference 50 kGy(tissue) (kV/in)
1	1	-0.2 (0.01)	-0.06 (0.004)	-0.2 (0.01)	-0.009 (0.004)
	2 + 3	0.05 (0.03)	-0.08 (0.002)	0.9 (0.03)	0.1 (0.002)
	4	0.04 (0.02)	0.004 (0.03)	0.05 (0.02)	0.02 (0.03)
2	1	-0.03 (0.007)	-0.04 (0.006)	0.08 (0.007)	-0.01 (0.007)
	2	-0.04 (0.008)	-0.004 (0.006)	0.07 (0.008)	-0.01 (0.006)
	3	0.04 (0.009)	-0.05 (0.005)	0.07 (0.009)	-0.06 (0.005)
	4	-0.1 (0.01)	0.09 (0.02)	-0.1 (0.01)	0.06 (0.02)
	5	0.01 (0.006)	0.05 (0.008)	0.0 (0.006)	0.2 (0.008)

Table 3-5. Electrostatic potential measurement of various layers within respirators. Standard deviation given in parenthesis.

Models	Layer	Average 0 kGy(tissue) (V)	Average 50 kGy(tissue) (V)
1	1	-78.6 (51.2)	-722 (246)
	2	-855 (453)	-809 (316)
	3	953 (208)	-1030 (251)
	4	1.44 (1.88)	0.90 (1.10)
2	1	167 (145)	-301 (157)
	2	-1890 (544)	-503 (310)
	3	2030 (369)	-964 (285)
	4	-384 (143)	484 (112)
	5	-4.20 (5.59)	3.36 (2.88)

3.5. Filtration Performance Testing

Both filtration systems produced similar results on the Model 2 respirators. Efficiency tests for the Model 1 respirator are reported below (Table 3-6) for the challenge particle size of 75 nm. The Model 2 respirator data for the large-scale filtration bed are shown in **Error! Reference source not found.**.

Table 3-6 Respirator facial respirator filter efficiency measurements with particulate size 75nm. Standard deviation given in parenthesis.

Models	kGy (tissue)	Machine	Filter Face Velocity (cm/s)	Efficiency at 75nm particle size (%)
1	0	A	17.337 (high)	99.31 (0.11)
	0	A	6.119 (low)	99.31 (0.15)
	25	A	17.337 (high)	57.25 (4.95)
	0	A	17.337 (high)	98.80 (0.16)
	25	A	17.337 (high)	53.53 (5.62)

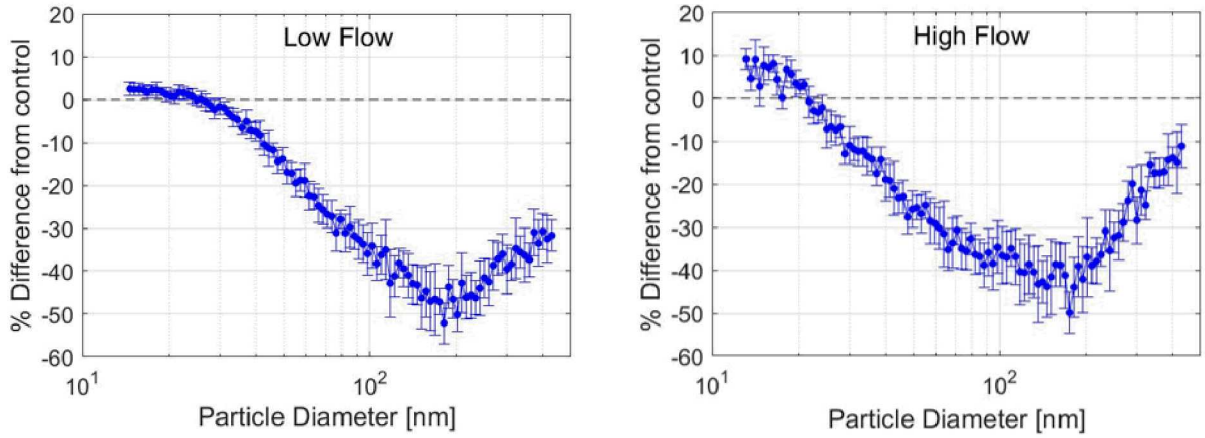

Figure 3-10. % Reduction in efficiency of 25 kGy(tissue) Model 2 respirator when compared to control part

These results show that gamma irradiation reduces the ability of electret based respirators to filter intermediate sized particles.

4. CONCLUSION

N95 filtering facepiece respirators use various mechanisms to capture and filter particles and bioaerosols from the air. QNFT performed in this study captured the combination of filtration efficacy, seal integrity and correct donning in evaluating respirator performance. Both respirator models had a statistically significant decrease in QNFT fit factor score after irradiation; however this effect is much more pronounced in the Model 1 respirator.

The collective of tests performed on the respirators revealed that gamma radiation can modify the electrostatic charge on the filter and measuring this change coincided with a decrease in QNFT fit factor score and a decrease in aerosol filtering efficiency around the 200 nm particle size.

Although gamma irradiation is a well-known technique for medical sterilization, it is beneficial to test PPE before using gamma radiation as a sterilization mode. The respirators were degraded in performance, but had no significant visual, or tactile indicators of the degradation. The quantitative tests in this study are useful for identifying that degradation has occurred.

N95 respirator models that are being considered for reuse after gamma sterilization should first be evaluated for post-radiation efficacy.

FUNDING AND DISCLOSURE STATEMENT

Manuscript transmitted on 5-20-2020; approved for unclassified, unlimited release under SAND2020-5274. Sandia National Laboratories is a multimission laboratory managed and operated by National Technology & Engineering Solutions of Sandia LLC, a wholly owned subsidiary of Honeywell International Inc. for the U.S. Department of Energy's National Nuclear Security Administration under contract DE-NA0003525. This work was funded by the Laboratory Directed Research and Development (LDRD) program at Sandia National Laboratories.

The authors declare no competing financial interests.

AUTHOR AFFILIATIONS

Sandia National Laboratories, Albuquerque, NM, USA

REFERENCES

1. CDC. Decontamination and Reuse of Filtering Facepiece Respirators. 2020 [Available from: https://www.cdc.gov/coronavirus/2019-ncov/hcp/ppe-strategy/decontamination-reuse-respirators.html.
2. Davies A, Thompson K-A, Giri K, Kafatos G, Walker J, Bennett A. Testing the efficacy of homemade masks: would they protect in an influenza pandemic? Disaster medicine and public health preparedness. 2013;7(4):413-8.
3. FDA. FAQs on 3D Printing of Medical Devices, Accessories, Components, and Parts During the COVID-19 Pandemic. 2020 [Available from: https://www.fda.gov/medical-devices/3d-printing-medical-devices/faqs-3d-printing-medical-devices-accessories-components-and-parts-during-covid-19-pandemic.
4. International Organization for Standardization. Sterilization of health care products - Radiation- Part 2: Establishing the sterilization dose (11137-2). 2013.
5. Cramer A, Tian E, Yu SH, Galanek M, Lamere E, Li J, et al. Disposable N95 Masks Pass Qualitative Fit-Test But Have Decreased Filtration Efficiency after Cobalt-60 Gamma Irradiation. medRxiv. 2020.
6. Feldmann F, Shupert WL, Haddock E, Twardoski B, Feldmann H. Gamma irradiation as an effective method for inactivation of emerging viral pathogens. The American journal of tropical medicine and hygiene. 2019;100(5):1275-7.
7. Viscusi DJ, Bergman M, Sinkule E, Shaffer RE. Evaluation of the filtration performance of 21 N95 filtering face piece respirators after prolonged storage. American journal of infection control. 2009;37(5):381-6.
8. Harrell CR, Djonov V, Fellabaum C, Volarevic V. Risks of using sterilization by gamma radiation: the other side of the coin. International journal of medical sciences. 2018;15(3):274.
9. Gamma Irradiation Facility and Low-Dose-Rate Irradiation Facility Sandia National Laboratories. 2020 [Available from: https://www.sandia.gov/research/facilities/gamma_irradiation_facility.html.
10. CDC. Laboratory performance evaluation of N95 filtering facepiece respirators, 1996. MMWR. 1998;47(48):1045.
11. OSHA. Fit Testing Procedures (Mandatory). Occupational Safety and Health Standards. 2004;1910.134 App A.
12. Wilkinson IJ, Pisaniello D, Ahmad J, Edwards S. Evaluation of a large-scale quantitative respirator-fit testing program for healthcare workers: survey results. Infection Control & Hospital Epidemiology. 2010;31(9):918-25.
13. Fisher EM, Shaffer RE. Considerations for recommending extended use and limited reuse of filtering facepiece respirators in health care settings. Journal of occupational and environmental hygiene. 2014;11(8):D115-D28.
14. CDC. Recommended Guidance for Extended Use and Limited Reuse of N95 Filtering Facepiece Respirators in Healthcare Settings. 2020 [Available from: https://www.cdc.gov/niosh/topics/hcwcontrols/recommendedguidanceextuse.html.
15. He X, Reponen T, McKay RT, Grinshpun SA. Effect of particle size on the performance of an N95 filtering facepiece respirator and a surgical mask at various breathing conditions. Aerosol Science and Technology. 2013;47(11):1180-7.
16. Walsh D, Stenhouse J. Parameters affecting the loading behavior and degradation of electrically active filter materials. Aerosol Science and Technology. 1998;29(5):419-32.

17. National Institute for Occupational Safety and Health. Determination of particulate filter efficiency level for N95 series filters against solid particulates for non-powered, air-purifying respirators standard testing procedure (STP). 2019: Procedure no. TEB-APR-STP-0059 Rev. 3.2.
18. Liu Y, Ning Z, Chen Y, Guo M, Liu Y, Gali NK, et al. Aerodynamic analysis of SARS-CoV-2 in two Wuhan hospitals. Nature. 2020.
19. Liu J, Zhang H, Gong H, Zhang X, Wang Y, Jin X. Polyethylene/polypropylene bicomponent spunbond air filtration materials containing magnesium stearate for efficient fine particle capture. ACS applied materials & interfaces. 2019;11(43):40592-601.

APPENDIX A. ADDITIONAL IMAGES

A.1. Model 1 Respirator Images

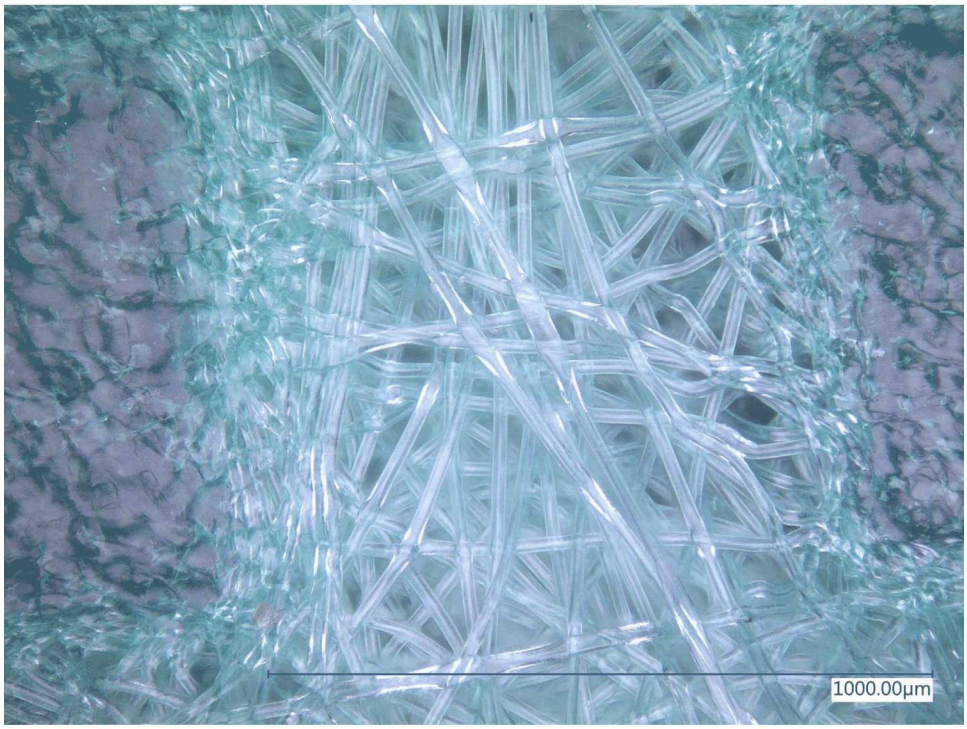

Figure A-1. Model 1 N95 Layer 1 250x 0 kGy(tissue)

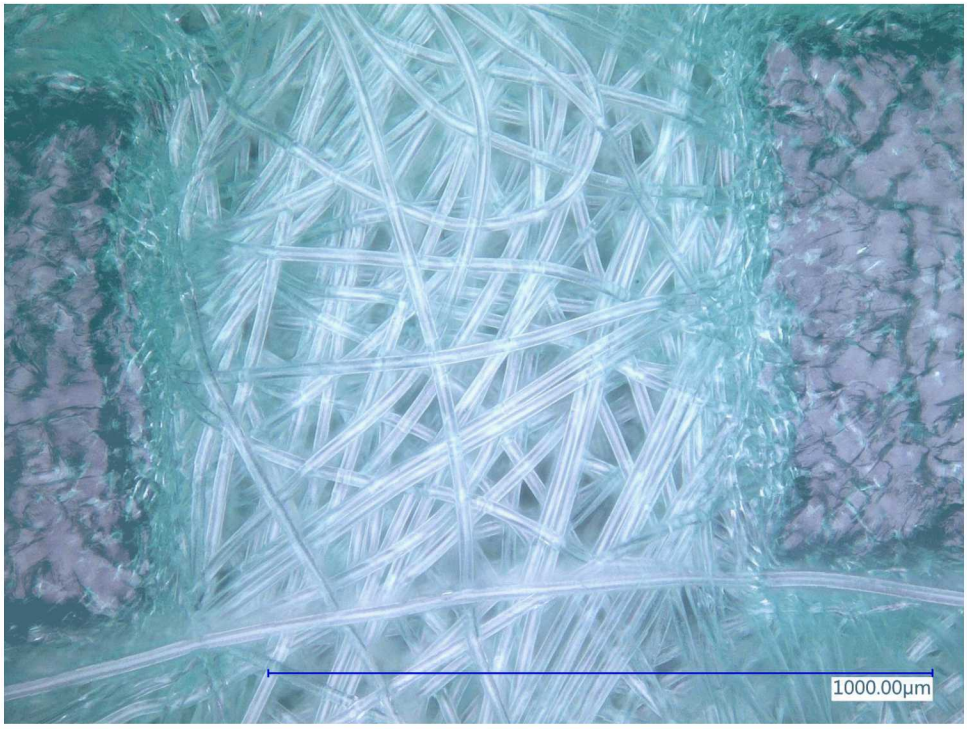

Figure A-2. Model 1 N95 Layer 1 250x 50 kGy(tissue)

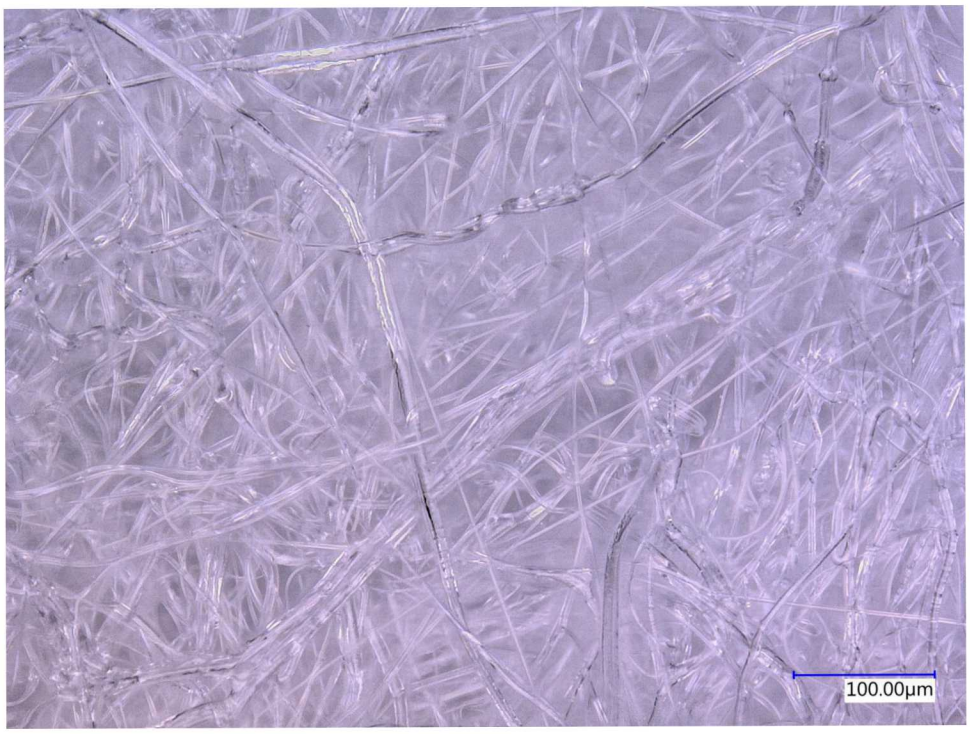

Figure A-3. Model 1 N95 Layer 2 500x 0 kGy(tissue)

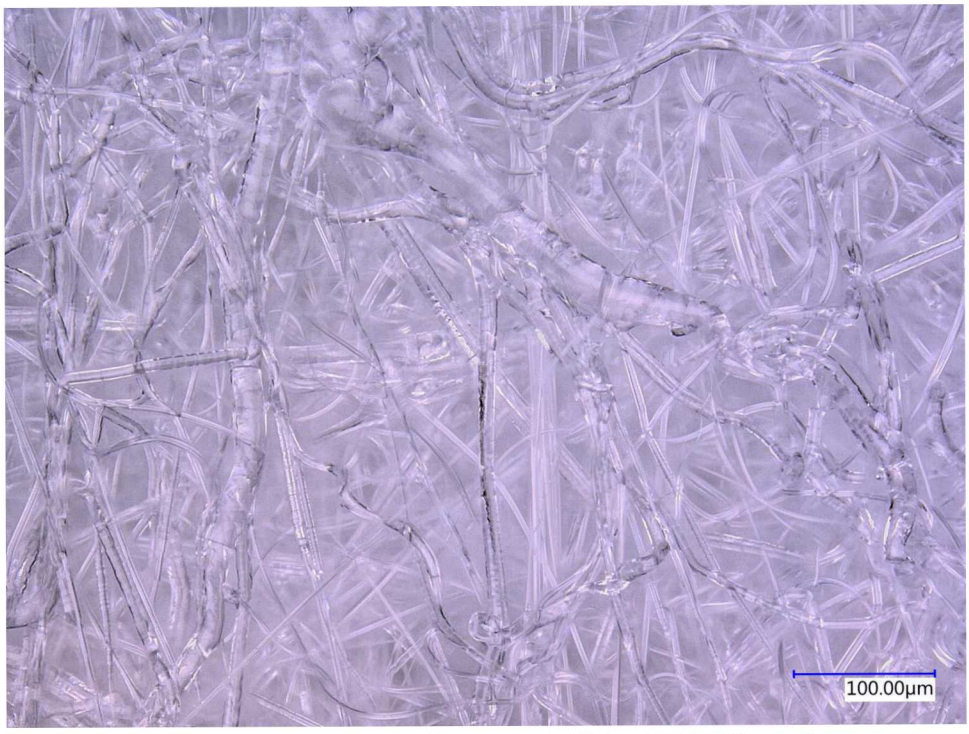

Figure A-4. Model 1 N95 Layer 2 500x 50 kGy(tissue)

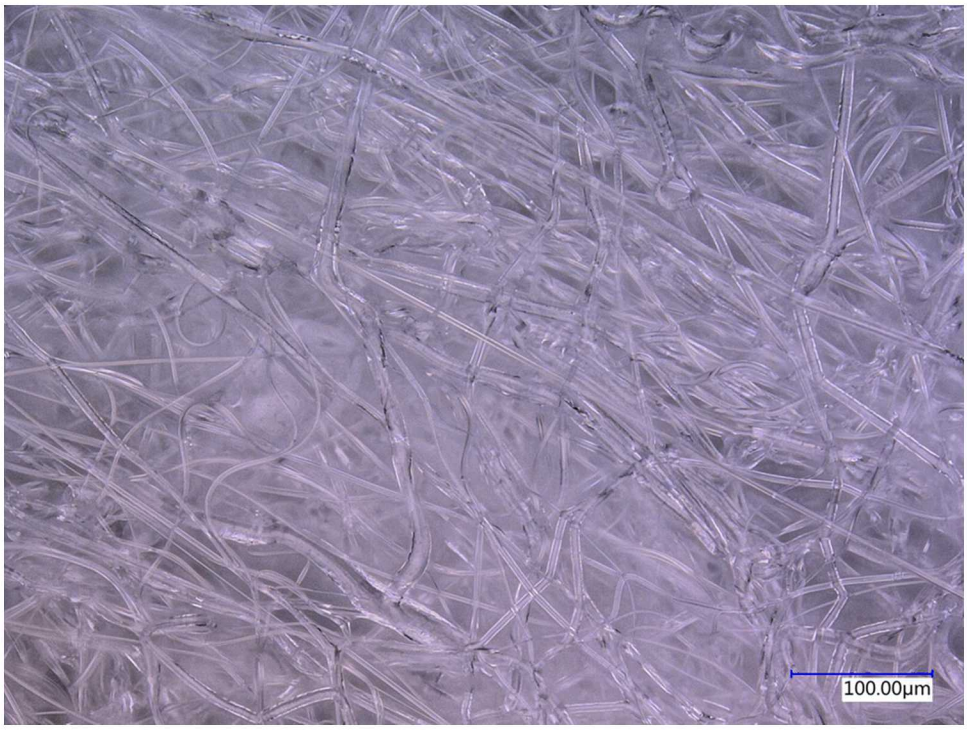

Figure A-5. Model 1 N95 Layer 3 500x 0 kGy(tissue)

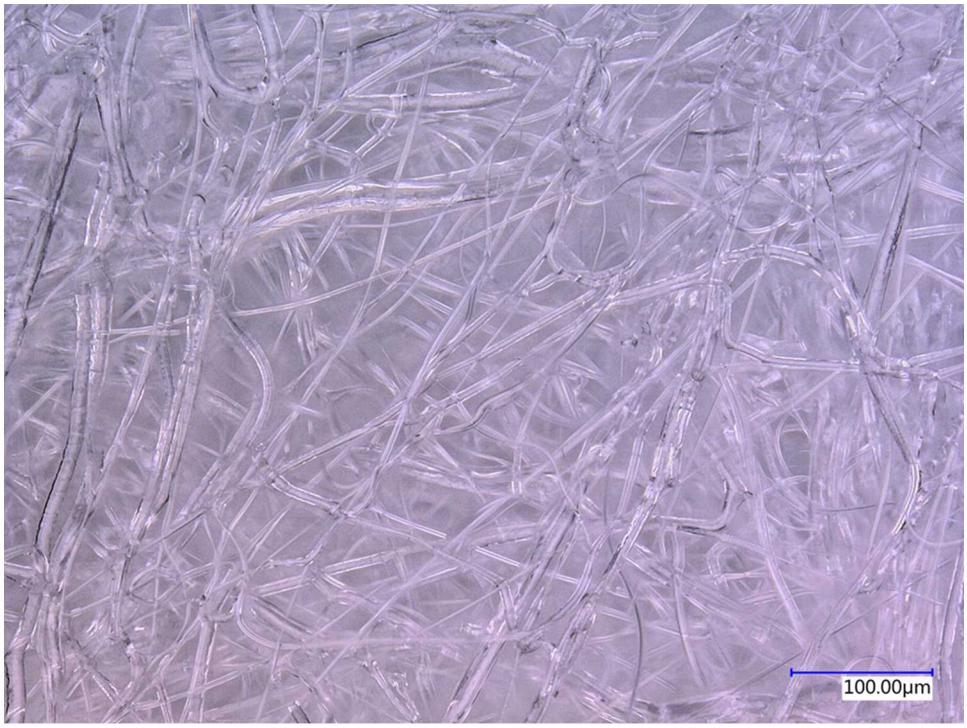

Figure A-6. Model 1 N95 Layer 3 500x 50 kGy(tissue)

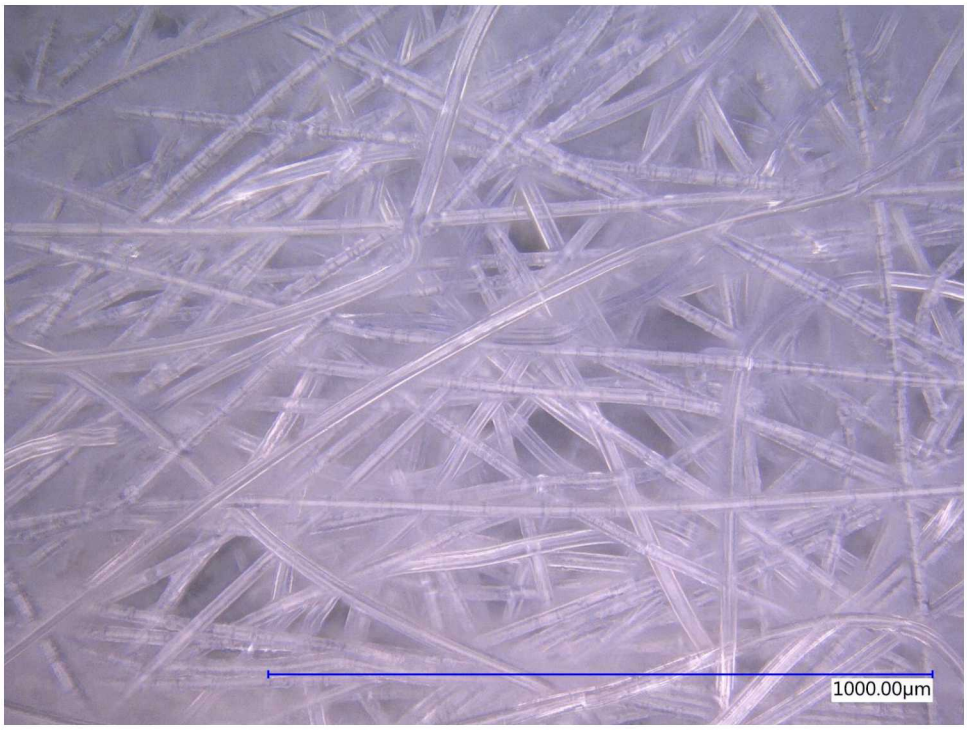

Figure A-7. Model 1 N95 Layer 4 250x 0 kGy(tissue)

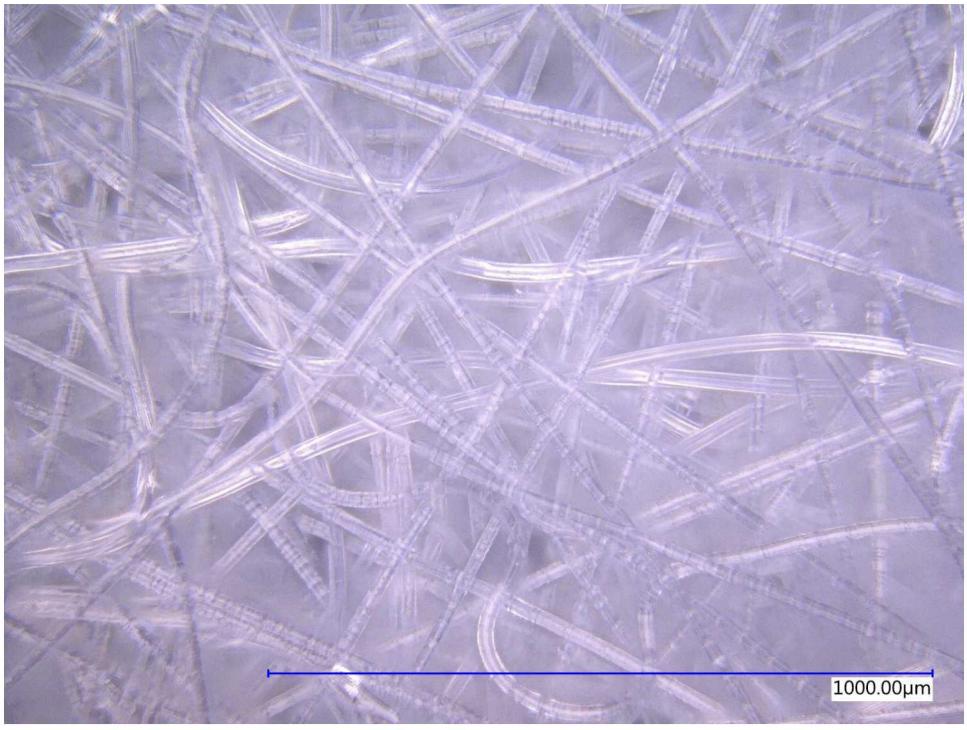

Figure A-8. Model 1 N95 Layer 4 250x 50 kGy(tissue)

A.2. Model 2 Respirator Images

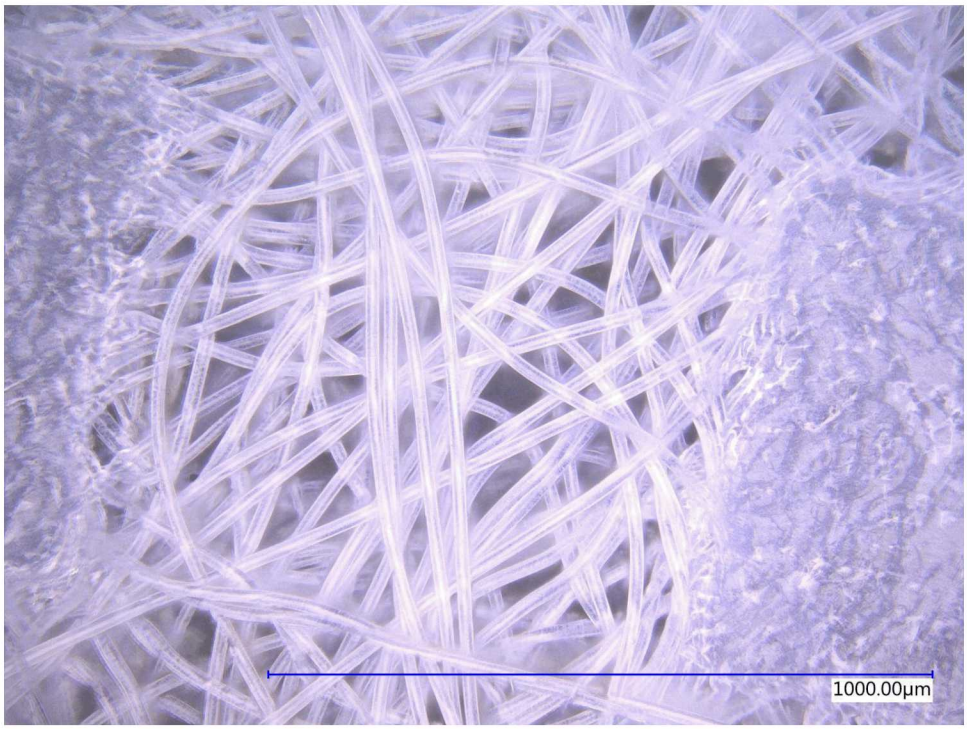

Figure A-9. Model 2 N95 Layer 1 250x 0 kGy(tissue)

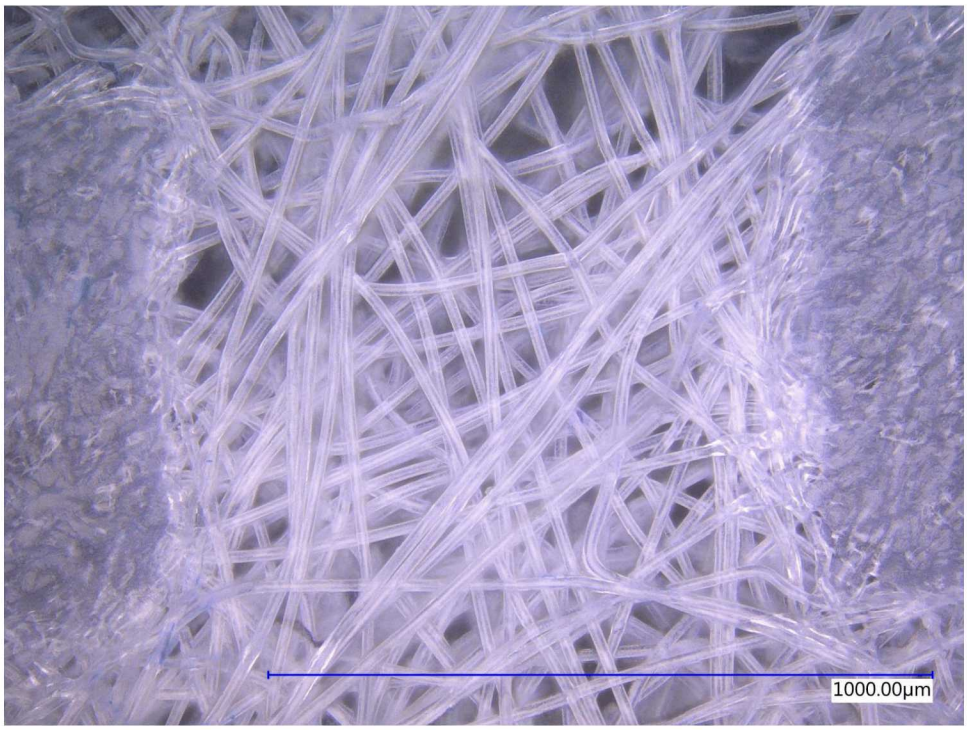

Figure A-10. Model 2 N95 Layer 1 250x 50 kGy(tissue)

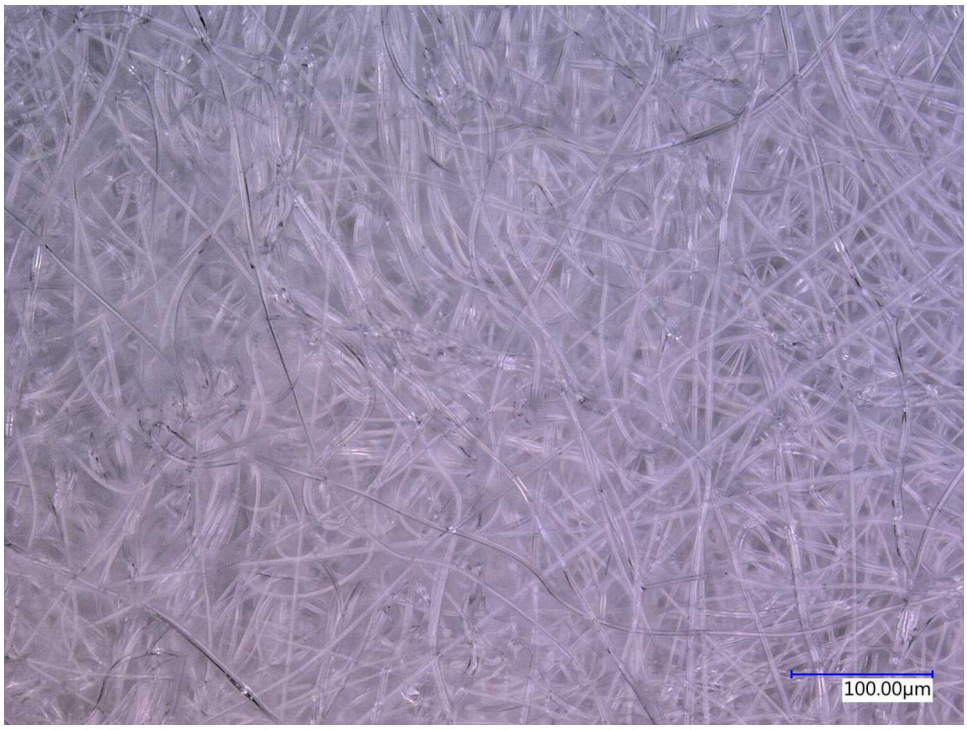

Figure A-11. Model 2 N95 Layer 2 500x 0 kGy(tissue)

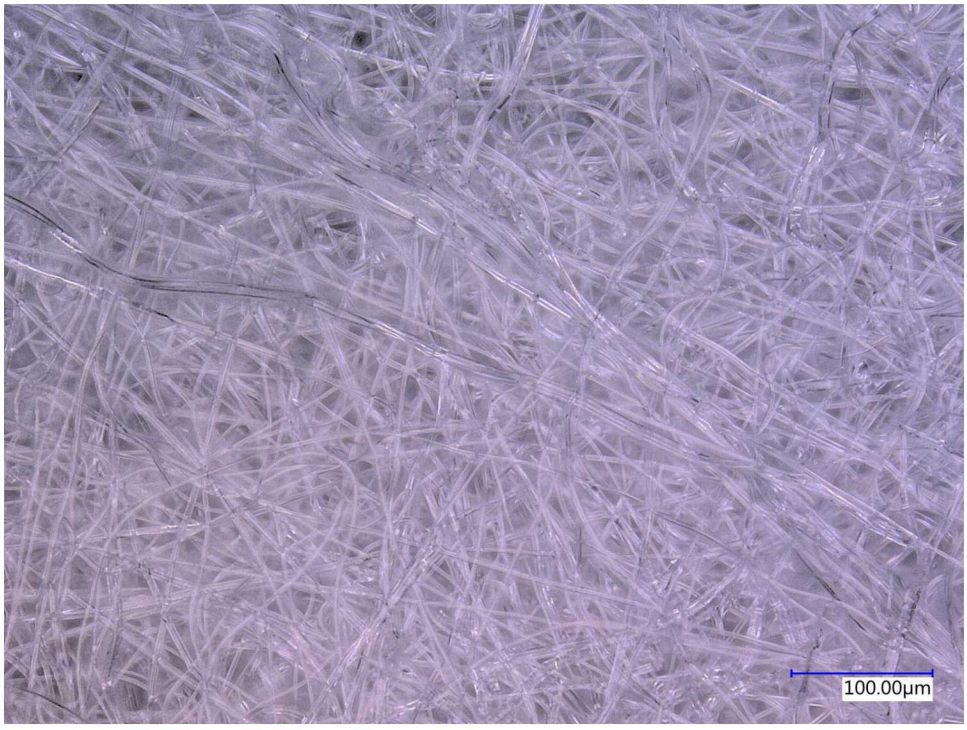

Figure A-12. Model 2 N95 Layer 2 500x 50 kGy(tissue)

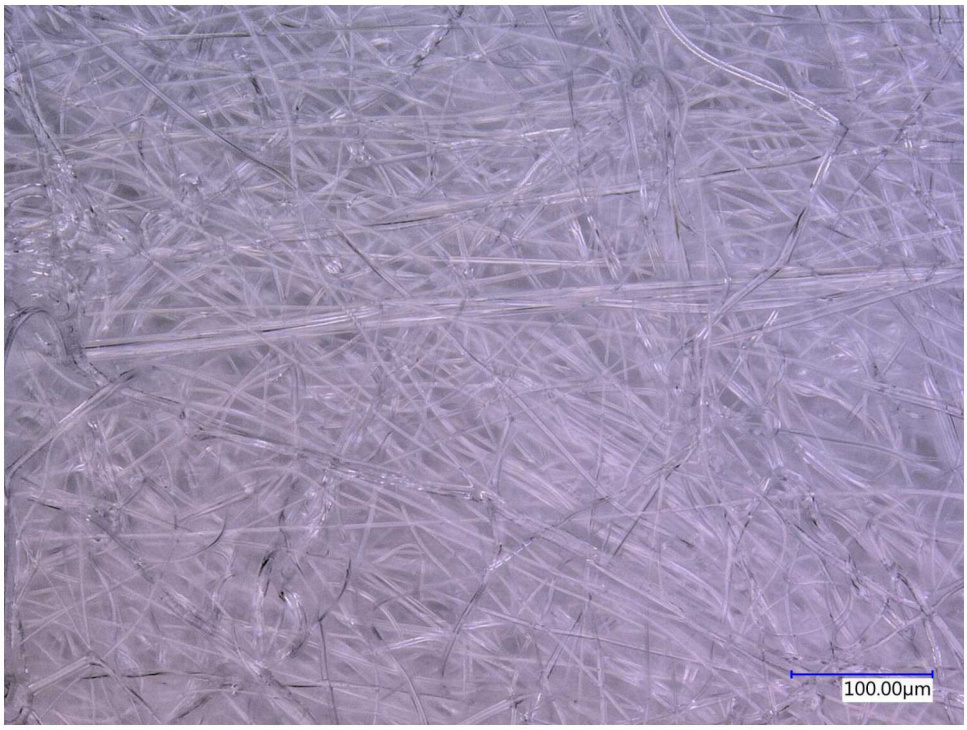

Figure A-13. Model 2 N95 Layer 3 500x 0 kGy(tissue)

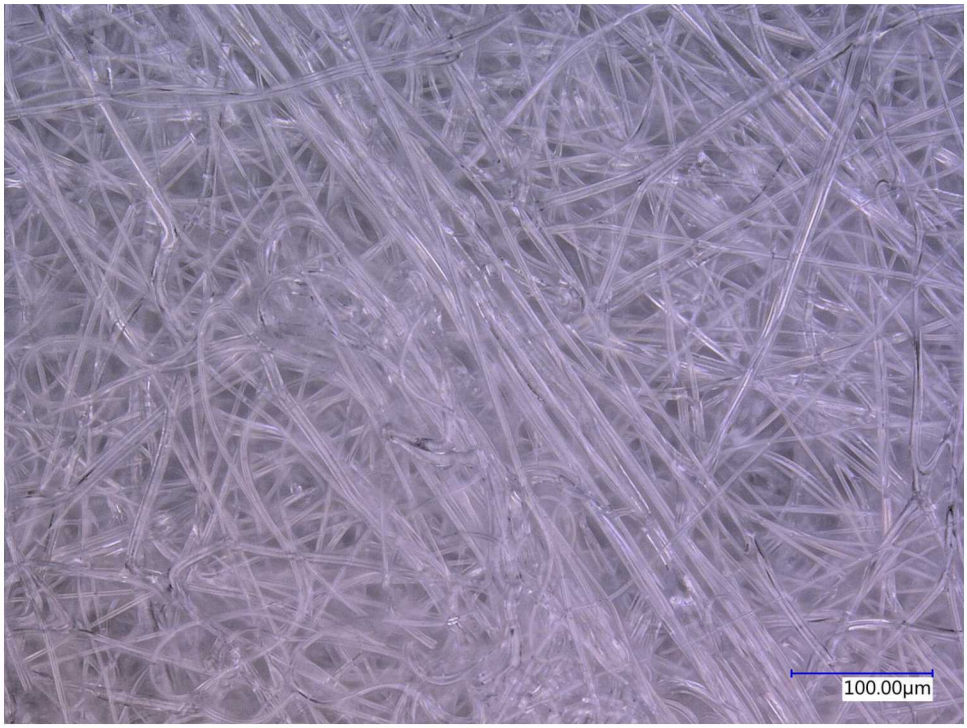

Figure A-14. Model 2 N95 Layer 3 500x 50 kGy(tissue)

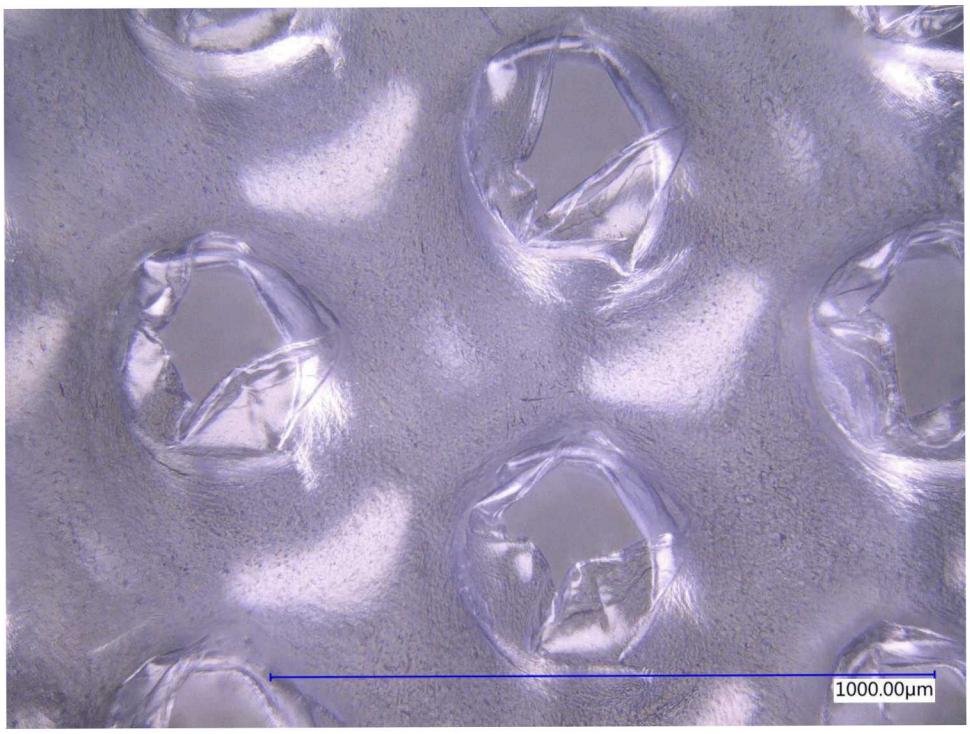

Figure A-15. Model 2 N95 Layer 4 250x 0 kGy(tissue)

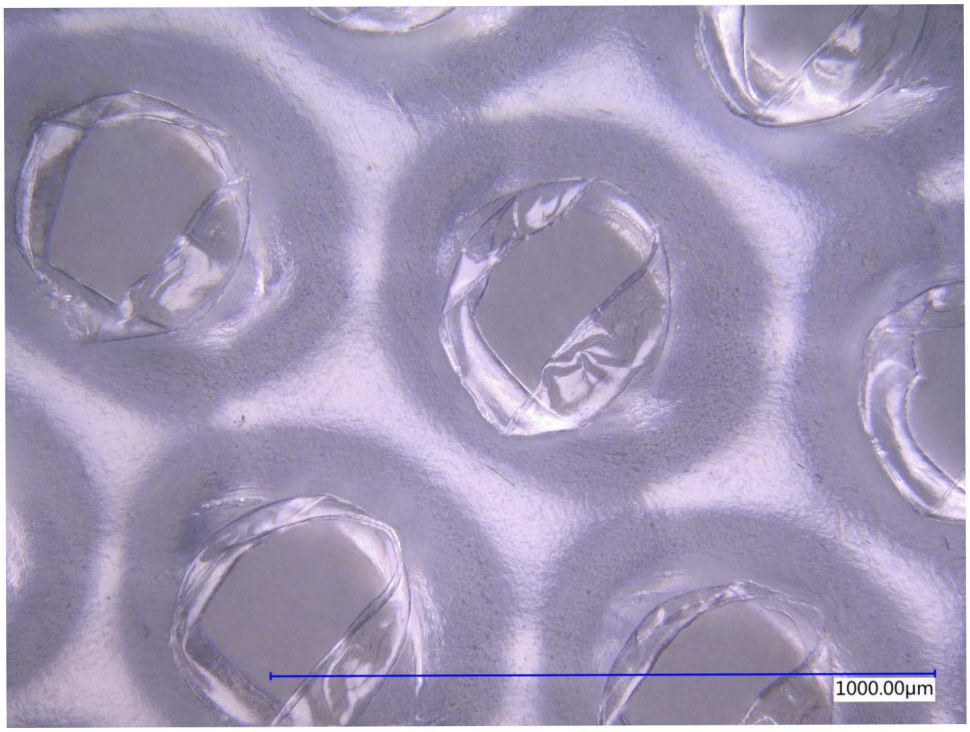

Figure A-16. Model 2 N95 Layer 4 250x 50 kGy(tissue)

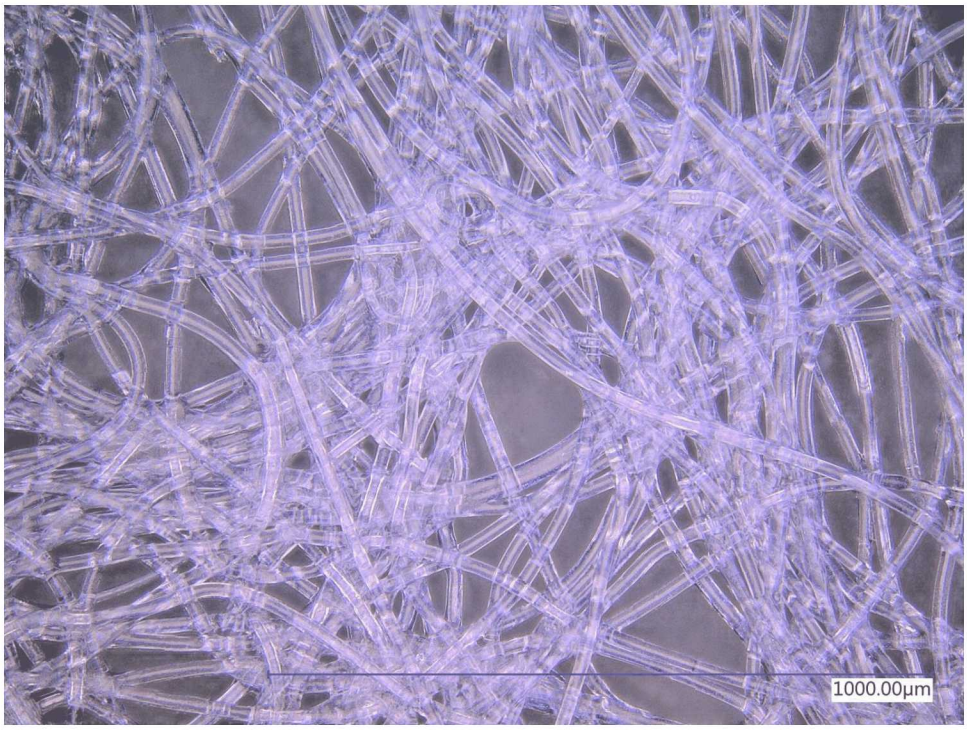

Figure A-17. Model 2 N95 Layer 5 250x 0 kGy(tissue)

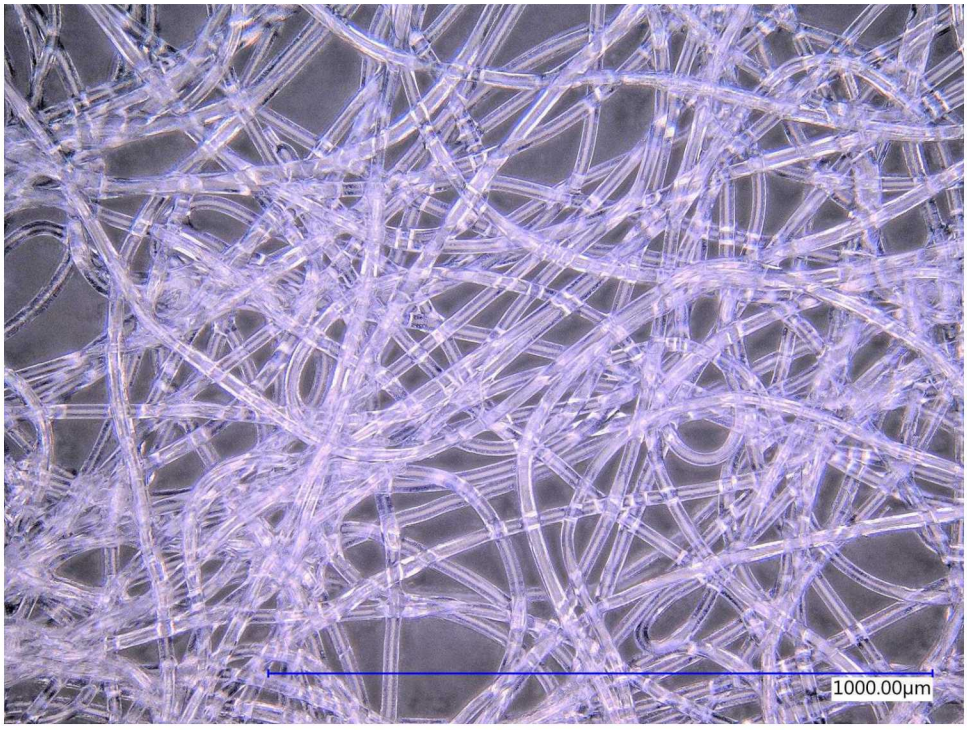

Figure A-18. Model 2 N95 Layer 5 250x 50 kGy(tissue)

DISTRIBUTION

Email—Internal

Name	Org.	Sandia Email Address
Technical Library	01977	sanddocs@sandia.gov

This page left blank

This page left blank

Sandia National Laboratories

Sandia National Laboratories is a multimission laboratory managed and operated by National Technology & Engineering Solutions of Sandia LLC, a wholly owned subsidiary of Honeywell International Inc. for the U.S. Department of Energy's National Nuclear Security Administration under contract DE-NA0003525.